Sustainable Production and In-place Utilization of a Liquid Nitrogenous Fertilizer

Kaiwen Yang
  Tianjin University

Shuhe Han
  Tianjin University

Yuting Wang (✉ wangyuting@tju.edu.cn)
  Tianjin University   https://orcid.org/0000-0001-6557-3537

Yifu Yu (✉ yyu@tju.edu.cn)
  Tianjin University   https://orcid.org/0000-0002-7927-1350

Bin Zhang (✉ zhanglab@tju.edu.cn)
  Tianjin University   https://orcid.org/0000-0003-0542-1819

Abstract

Efficient production and utilization of nitrogenous fertilizers can increase the food supply to support the dramatic increase of world's population. However, the conventional centralized production and excessive use of solid nitrogenous fertilizers leads to severe waste and environmental pollution. The adoption of liquid nitrogenous fertilizer can maximize the utilization efficiency. Since plants can simultaneously absorb ammonium- and nitrate-nitrogen fertilizer, herein, we propose a two-step relay strategy to sustainably produce NH_4NO_3 solution for in-place utilization by using air and water as raw materials. This distributed synthesis approach can be easily incorporated into present irrigation systems with controllable fertilizer concentrations for different crops. Furthermore, a techno-economic analysis is conducted to confirm the application potential of this strategy. This perspective provides new insight for the sustainable production and in-place utilization of liquid nitrogenous fertilizers at appropriate concentrations and hopefully promotes the development of smart agriculture.

Context & Scale

Population expanding has brought global food scarcity. Nitrogenous fertilizer is vital to increase the food supply. The centralized production of nitrogenous fertilizer requires huge energy consumption and fixed assets investment. Presently, the global energy problem further aggravates nitrogenous-fertilizer crisis, especially in developing countries. Moreover, the use of solid nitrogenous fertilizers leads to a severe waste (utilization rate < 50%), resulting in underground water pollution.

Herein, we exhibit a two-step relay strategy for distributed production and in-place utilization of liquid NH4NO3 fertilizer, namely, the plasma-driven air-to-NOx conversion, and then electrocatalytic conversion to produce NH4NO3. The whole process can be driven by volatile green energy such as wind and solar power. A cost-effective techno-economic analysis for liquid NH4NO3 production is provided, proving the application potential of the two-step relay strategy for nitrogenous fertilizers supply.

INTRODUCTION

Nitrogenous fertilizer, as the largest consumed chemical fertilizer, has increased food production to support ~ 40% of the world's population.[1] In this regard, the Haber-Bosch (H-B) method for nitrogen fixation has been considered the greatest invention in the 20th century.[2] In conventional agriculture, solid nitrogenous fertilizer is produced in centralized chemical plants and then transported to where it is needed. Both processes are highly dependent on fossil fuels with the emission of huge amounts of greenhouse gas. Moreover, the utilization rate of the applied solid nitrogenous fertilizer is less than 50%,[3] inevitably leading to diffusion of unabsorbed nitrogenous fertilizer into underground water. Very recently, the introduction of liquid fertilizer into precision irrigation systems was proven to significantly improve fertilizer use efficiency.[4] Thus, the development of new routes for distributed production and in-place utilization of liquid nitrogenous fertilizer driven by renewable energy is of great significance.

Since plants can simultaneously absorb ammonium- and nitrate-nitrogen fertilizer, ammonium nitrate (NH_4NO_3) solution can serve as a good candidate carbon-free liquid nitrogenous fertilizer.[5] Herein, we exhibit a two-step relay strategy to sustainably produce NH_4NO_3 solution by using air and water as raw materials (Fig. 1). In the first step, air is converted into NO_x by plasma technology. In the second step, the produced NO_x is dissolved in water and then converted to NH_4NO_3 solution by electrocatalytic reduction. Both steps can be directly driven by volatile green energy such as wind and solar power. The NH_4NO_3 solution produced by this distributed two-step relay strategy can be easily integrated into the present precision irrigation system with controllable fertilizer concentrations for different crops. We summarized the significant progress in plasma-driven air-to-NO_x conversion and electrocatalytic NO_x^- reactions.[6,7] Surprisingly, the two-step relay strategy has gained an economic advantage over conventional manufacturing for solid NH_4NO_3 fertilizer based on techno-economic analysis (TEA). This work offers a method for sustainable production and in-place utilization of liquid nitrogenous fertilizer with high use efficiency, assisting the development of smart agriculture.
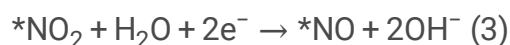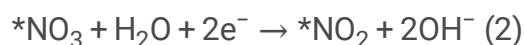
STEP 1: PLASMA-DRIVEN AIR-TO-NO_x CONVERSION

Nitrogen fixation to form nitrogen-containing oxides (NO_x/NO_x^-) can be driven by light irradiation, electricity and plasma.[7,8] In 1989, O. A. Ileperuma et al. [9] showed that TiO_2-coated ZnO dispersed in an aqueous solution could convert nitrogen to nitrate under ultraviolet radiation. Recently, photocatalytic air conversion for NO_x synthesis was developed by our group.[10] In addition, a direct electrochemical nitrogen oxidation strategy to form NO_3^- was mentioned by Chen et al.[11] and experimentally proven by our group[12] in 2019. Although great efforts have been devoted to this area, the efficiency of NO_x/NO_x^- synthesis via photo/electrocatalytic nitrogen oxidation is still very low because of the difficulty in activating the strong $N \equiv N$ bond (941 kJ mol^{-1}).[13] In contrast, plasma-driven nitrogen fixation has been considered an attractive technology due to its high efficiency in nitrogen activation.[14] The plasma process, as one of the oldest phenomena occurring on Earth (e.g., lightning), is generated by the ionization of gases. The first industrial application of atmospheric nitrogen fixation was known as the Birkeland-Eyde (B-E) plasma process.[15] Specifically, plasma arcs were generated in the thermal-plasma furnace, and then the air passed the furnace to combust and produce NO_x. It was reported that only ~ 3% of input energy was utilized in the B-E process for NO_x production. Although several improvement methods, such as waste heat utilization from process gases and the operation of furnaces at high pressure, have been developed, the energy efficiency is still unsatisfactory. Moreover, the NO_x products tended to dissociate when not supplied to thermal quenching.[15]

Instead, non-thermal plasma is taking the dominant status due to its low theoretical energy consumption for nitrogen fixation (approximately 0.2 MJ mol^{-1}-N) and easy operation at low temperature.[14] In a typical non-thermal plasma reactor, the bulk temperature remains ambient, while the temperature of internal electrons can exceed several thousands of K, which allows for selective activation of the $N \equiv N$

bond.[16,17] Based on different discharge patterns, non-thermal plasma can be divided into dielectric barrier discharge (DBD) plasma, glow discharge plasma, microwave (MW) plasma, gliding arc discharge plasma and so on. Figure 2a and Supplementary Table S1 summarize the progress on non-thermal plasma-driven NO_x synthesis with respect to plasma types, operation parameters and energy costs. For example, DBD plasma coupled with catalysts was able to achieve nitrogen fixation with an energy cost of 18 MJ mol^{-1}-N.[18] Pei et al.[19] reduced the specific energy cost for NO_x formation to ~ 2.8 MJ mol^{-1}-N by adopting direct current glow discharge at atmospheric pressure. The value was further reduced to 2.0 MJ mol^{-1}-N for an electrode-free MW plasma because electrode-free ignition could effectively reduce energy loss to the walls.[20] Notably, Patil et al.[21] employed gliding arc discharge plasma to prepare NO_x with 1% concentration at an energy cost of 1.43 MJ mol^{-1}-N. It allowed the generation of higher NO_x concentrations by increasing the frequency, pulse width, and amplitude.
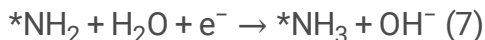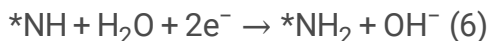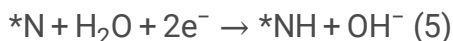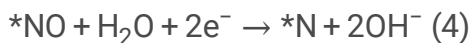
STEP 2: ELETRO-CATALYTIC NITRATE-TO-AMMONIA CONVERSION

The obtained NO_x (NO_2/NO) from the plasma process firstly get through aqueous solution. NO is insoluble in water, and NO_2 reacts with water to form nitrate and NO. With the presence of O_2, the produced NO_x finally dissolves in the electrolyte to form nitrate. Thus, the second step in the relay strategy is the electrocatalytic reduction of half nitrate to form NH_4NO_3 solution. The rational design and optimization of electrocatalysts with maximum efficiency and selectivity for ammonia requires a fundamental understanding of the reaction mechanism.[6,22] The process of the electrochemical nitrate reduction reaction (NO_3RR) can be summarized as the deoxidation and hydrogenation of nitrogen-containing intermediates, involving the transfer of eight electrons and nine protons. [28,30,31] There are many stable intermediates with various valence states, including NO_2, NO, N_2O, N_2 and NH_2OH, which can escape from the catalyst surface as products. Although the thermodynamic equilibrium potential of each intermediate varies considerably, many intermediates may coexist in the actual catalytic process due to the specific kinetic processes and the differences in their adsorption energy.[23] As a result, there is selective competition for the production of any target product.[24] The reaction pathway of the NO_3RR begins with the adsorption of nitrate to the active site and its gradual deoxidation process. This process can be summarized by equations (1)−(3).

$*NO_3^- \rightarrow *NO_3 + e^-$ (1)

$*NO_3 + H_2O + 2e^- \rightarrow *NO_2 + 2OH^-$ (2)
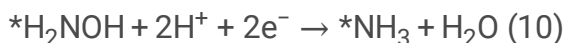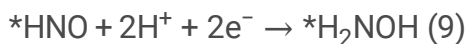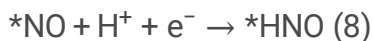
$*NO_2 + H_2O + 2e^- \rightarrow *NO + 2OH^-$ (3)

Next, the resulting *NO intermediate is hydrogenated. The mechanism of N-O bond cleavage can be divided into direct breaking followed by hydrogenation and successive hydrogenation followed by dehydration.

Direct breaking followed by hydrogenation model:

$$*NO + H_2O + 2e^- \rightarrow *N + 2OH^- \quad (4)$$

$$*N + H_2O + 2e^- \rightarrow *NH + OH^- \quad (5)$$

$$*NH + H_2O + 2e^- \rightarrow *NH_2 + OH^- \quad (6)$$

$$*NH_2 + H_2O + e^- \rightarrow *NH_3 + OH^- \quad (7)$$

Successive hydrogenation followed by dehydration model:

$$*NO + H^+ + e^- \rightarrow *HNO \quad (8)$$

$$*HNO + 2H^+ + 2e^- \rightarrow *H_2NOH \quad (9)$$

$$*H_2NOH + 2H^+ + 2e^- \rightarrow *NH_3 + H_2O \quad (10)$$

In equations (4)−(7), if two *N intermediates couple, a byproduct of N_2 will be generated. In equations (8)−(10), $*NH_2OH$ might be generated as a byproduct. Different hydrogenation pathways produce different intermediates and byproducts.[25] Therefore, it is crucial to design electrocatalysts with high activity and selectivity toward the synthesis of goal products from the NO_3RR.[23,26] Here, we summarized various types of catalysts for the NO_3RR, including metal-free electrocatalysts, transition metal-based electrocatalysts, and noble metal-based electrocatalysts (Fig. 2b and Supplementary Table S2). Metal-free eletrocatalysts are represented by carbon-based materials. Polymeric carbon nitride with a controlled number of nitrogen vacancies exhibited 90% Faradaic efficiency (FE) and 0.03262 mmol g^{-1} h^{-1} yield for ammonia product at -0.75 V versus reversible hydrogen electrode (RHE).[27] Transition metal-based catalysts have long been the focus of research in electrocatalysis due to their low cost, high activity, and potential for large-scale applications. Cobalt phosphide (CoP) nanosheets with a three-dimensional structure exhibited ~ 100% FE and a 9.56 mol h^{-1} m^{-2} yield of ammonia at a potential of -0.3 V vs. RHE.[28] Compared to metallic cobalt nanosheets, the introduction of phosphorus atoms into the lattice effectively stabilized the active phase and optimized the energy barriers of the key steps in the NO_3RR. Sargent et al.[29] prepared a series of CuNi alloys with various Cu:Ni compositions by electrodeposition, which electrochemically reduced nitrate into ammonia with a FE of 99 ± 1% and a yield of 0.48 mmol h^{-1} cm^{-2} at -0.15 V vs. RHE. With increasing Ni content in the CuNi alloys, the *d*-band center of Cu upshifted, and the anti-bonding occupation decreased, which greatly enhanced the intermediate adsorption energy. Noble metal-based catalysts with empty *d*-orbitals have been considered state-of-the-art electrocatalysts for the NO_3RR due to the role of *d*-orbital electrons in enhancing charge injection of the lowest vacancy molecular orbital of nitrate. Luo et al.[30] designed rhodium nanoflowers as NO_3RR electrocatalysts, in which the low-coordination Rh atoms facilitated the adsorption of nitrate ions and stabilized the

intermediates. As a result, this electrocatalyst reduced nitrate to ammonia with a 95% FE and 0.0149 mmol h^{-1} cm^{-2} yield at + 0.2 V vs. RHE. Very recently, we proposed a novel three-step relay mechanism to decrease the reaction overpotential for the NO$_3^-$RR. A series of Ru$_x$Co$_y$ catalysts were designed and prepared to perform the three-step relay mechanism, in which Ru$_{15}$Co$_{85}$ exhibited the optimal catalytic performance (onset potential: +0.4 V vs. RHE, FE: 96.8%, yield: 3.2 mol g$_{cat}^{-1}$ h^{-1}).[31] Moreover, great progress has been made in scaling up NO$_3$RR. An electrochemical system with a working volume of 500 L was used to electrochemically reduce nitrate to ammonia by Feng's group.[32] The selectivity of NH$_4^+$ in this system was over 92.0% with concentrations ranging from 241 mg L^{-1} to 2527 mg L^{-1}, and the productivity of NH$_4^+$ did not decay after 2 months of continuous operation. This proves the practical application potential of the NO$_3$RR to produce ammonia.

POTENTIAL ECONOMIC BENEFITS OF THE TWO-STEP RELAY STRATEGY

To ascertain the economic potential of the two-step relay strategy, we conduct a techno-economic analysis (TEA) based on the model reported recently.[33] The parameters used in the TEA are reasonably assumed according to the reported performances (Fig. 3, see details in Supplementary Information). The energy cost for plasma-driven NO$_x$ formation is chosen as 1.43 MJ mol^{-1} in the gliding arc plasma reactor at atmospheric pressure, and the energy efficiency (EE) of the Ru$_{15}$Co$_{85}$ catalyst was determined to be 41.54% for electrocatalytic nitrate reduction to ammonia.[21,31] The costs in the model are separated into three components, namely, the operating costs, the capital costs and other costs. Electricity costs take up the majority of the operation costs, in which the plasma process and electrochemical process occupy 49.46% and 22.48%, respectively. Notably, the TEA results indicate that the two-step relay strategy is profitable for NH$_4$NO$_3$ production (cost: 433 $ tonne^{-1}; market price: 500 $ tonne^{-1}).[34] In addition, the costs of this strategy will decrease rapidly along with the decrease of the energy consumption and the green electricity price, proving the promising application potential.

OPPORTUNITIES AND PERSPECTIVES

In summary, we propose a two-step relay strategy for distributed production and in-place utilization of liquid NH$_4$NO$_3$ fertilizer, that is, plasma-driven air-to-NO$_x$ conversion coupled with electrocatalytic conversion of nitrate to ammonia. The TEA shows that this route has commercial potential with an efficient integrated system in areas where renewable energy is abundant. However, there are still challenges in future applications. For the plasma process, the theoretical energy consumption for NO$_x$ synthesis is 0.2 MJ mol^{-1}, which is much less than the minimum energy consumption reported in the current literature[15]. Therefore, we must make an effort to improve the energy efficiency of non-thermal plasma. For example, when the electrode structure is optimized, it is possible to provide a higher electric field strength during discharge, reducing the breakdown voltage. The adoption of advanced catalysts in

plasma reactors can further improve the NO_x concentration. For electrochemical processes, a neutral electrolyte is indispensable for irrigation. However, presently reported NO_3RR catalysts usually exhibit high performance in alkaline electrolytes due to the suppression of the competition hydrogen evolution reaction. Thus, it is highly desirable to design and prepare efficient NO_3RR catalysts in neutral electrolytes. This perspective opens new opportunities to solve the global nitrogenous fertilizer crisis.

Declarations

AUTHOR CONTRIBUTIONS

Y.W., B.Z., and Y.Y. offered the idea. K.Y. and S.H. wrote the paper.

DECLARATION OF INTERESTS

The authors declare no conflict of interest.

References

1. Erisman, J.W., Sutton, M. A., Galloway, J., Klimont, Z., and Winiwarter, W. (2008). How a century of ammonia synthesis changed the world. Nature geoscience. Nat. Geosci. *1*, 636-639. https://doi.org/10.1038/ngeo325.

2. Wang, L., Xia, M., Wang, H., Huang, K., Qian, C., Maravelias, C.T., and Ozin, G.A. (2018). Greening Ammonia toward the Solar Ammonia Refinery. Joule *2*, 1055-1074. https://doi.org/10.1016/j.joule.2018.04.017.

3. Meena, V.S., Meena, S.K., Verma, J.P, Kumar, A., Aeron, A., Mishra, P.K., Bisht, J.K., Pattanayak, A., Naveed, M., and Dotaniya, M.L. (2017). Plant beneficial rhizospheric microorganism (PBRM) strategies to improve nutrients use efficiency: A review. Ecol. Eng. *107*, 8-32. https://doi.org/10.1016/j.ecoleng.2017.06.058.

4. Mikula, K., Izydorczyk, G., Skrzypczak, D., Mironiuk, M., Moustakas, K., Witek-Krowiak, A., and Chojnacka, K. (2020). Controlled release micronutrient fertilizers for precision agriculture - A review. Sci. Total Environ. *712*, 136365. https://doi.org/10.1016/j.scitotenv.2019.136365.

5. Riley, D., and Barber, S.A. (1971). Effect of Ammonium and Nitrate Fertilization on Phosphorus Uptake as Related to Root-Induced pH Changes at the Root-Soil Interface. Soil Sci Soc Am J *35*, 301-306. https://doi.org/10.2136/sssaj1971.03615995003500020035x.

6. Andersen, S.Z., Colic, V., Yang, S., Schwalbe, J.A., Nielander, A.C., McEnaney, J.M., Enemark-Rasmussen, K., Baker, J.G., Singh, A.R., Rohr, B.A., et al. (2019). A rigorous electrochemical ammonia synthesis protocol with quantitative isotope measurements. Nature *570*, 504-508. https://doi.org/10.1038/s41586-019-1260-x.

7. Li, L., Tang, C., Cui, X., Zheng, Y., Wang, X., Xu, H., Zhang, S., Shao, T., Davey, K., and Qiao, S.Z. (2021). Efficient Nitrogen Fixation to Ammonia through Integration of Plasma Oxidation with Electrocatalytic Reduction. Angew. Chem. Int. Ed. *60*, 14131-14137. https://doi.org/10.1002/ange.202104394.

8. Dai, C., Sun, Y., Chen, G., Fisher, A.C., and Xu, Z.J. (2020). Electrochemical Oxidation of Nitrogen toward Direct Nitrate Production on Spinel Oxides. Angew. Chem. Int. Ed. *59*, 9418-9422. https://doi.org/10.1002/anie.202002923.

9. Ileperuma, O.A., Weerasinghe, F. N. S., and Bandara, T. L. (1989). Photoinduced oxidative nitrogen fixation reactions on semiconductor suspensions. Sol. Energy Mater Sol. Cells *19*, 409-414. https://doi.org/10.1016/0165-1633(89)90035-X.

10. Yu, Y., Wang, C., Yu, Y., Huang, Y., Liu, C., Lu, S., and Zhang, B. (2020). A nitrogen fixation strategy to synthesize NO via the thermally assisted photocatalytic conversion of air. J. Mater. Chem. A *8*, 19623-19630. https://doi.org/10.1039/d0ta06747d.

11. Chen, J.G., Crooks, R.M., Seefeldt, L.C., Bren, K.L., Bullock, R.M., Darensbourg, M.Y., Holland, P.L., Hoffman, B., Janik, M.J., Jones, A.K., et al. (2018). Beyond fossil fuel-driven nitrogen transformations. Science *360*. https://doi.org/10.1126/science.aar6611.

12. Wang, Y., Yu, Y., Jia, R., Zhang, C., and Zhang, B. (2019). Electrochemical synthesis of nitric acid from air and ammonia through waste utilization. Natl. Sci. Rev. *6*, 730-738. https://doi.org/10.1093/nsr/nwz019.

13. Jacobsen, C.J., Dahl, S., Clausen, B. S., Bahn, S., Logadottir, A., and Nørskov, J. K. (2001). Catalyst design by interpolation in the periodic table: bimetallic ammonia synthesis catalysts. J. Am. Chem. Soc. *123*, 8404-8405. https://doi.org/10.1021/ja010963d.

14. Patil, B.S., Wang, Q., Hessel, V., and Lang, J. (2015). Plasma N_2-fixation: 1900−2014. Catal. Today, *256*, 49-66. https://doi.org/10.1016/j.cattod.2015.05.005.

15. Rouwenhorst, K.H.R., Jardali, F., Bogaerts, A., and Lefferts, L. (2021). From the Birkeland-Eyde process toward energy-efficient plasma-based NO_x synthesis: a techno-economic analysis. Energy Environ. Sci. *14*, 2520-2534. https://doi.org/10.1039/d0ee03763j.

16. Vervloessem, E., Aghaei, M., Jardali, F., Hafezkhiabani, N., and Bogaerts, A. (2020). Plasma-Based N_2 Fixation into NO_x: Insights from Modeling toward Optimum Yields and Energy Costs in a Gliding Arc Plasmatron. ACS Sustain. Chem. Eng. *8*, 9711-9720. https://doi.org/10.1021/acssuschemeng.0c01815.

17. He, L., Zhou, D., Lin, Y., Ge, R., Hou, X., Sun, X., and Zheng, C. (2018). Ultrarapid in Situ Synthesis of Cu_2S Nanosheet Arrays on Copper Foam with Room-Temperature-Active Iodine Plasma for Efficient and Cost-Effective Oxygen Evolution. ACS Catal. *8*, 3859-3864. https://doi.org/10.1021/acscatal.8b00032.

18. Patil, B.S., Cherkasov, N., Lang, J., Ibhadon, A.O., Hessel, V., and Wang, Q. (2016). Low temperature plasma-catalytic NO_x synthesis in a packed DBD reactor: Effect of support materials and supported active metal oxides. Appl. Catal. B *194*, 123-133. https://doi.org/10.1016/j.apcatb.2016.04.055.

19. Pei, X., Gidon, D., and Graves, D.B. (2019). Specific energy cost for nitrogen fixation as NO_x using DC glow discharge in air. J. Phys. D *53*. https://doi.org/10.1088/1361-6463/ab5095.

20. Kelly, S., and Bogaerts, A. (2021). Nitrogen fixation in an electrode-free microwave plasma. Joule *5*, 3006-3030. https://doi.org/10.1016/j.joule.2021.09.009.

21. Patil, B.S., Rovira Palau, J., Hessel, V., Lang, J., and Wang, Q. (2015). Plasma Nitrogen Oxides Synthesis in a Milli-Scale Gliding Arc Reactor: Investigating the Electrical and Process Parameters. Plasma Chem. Plasma Process. *36*, 241-257. https://doi.org/10.1007/s11090-015-9671-4.

22. van Langevelde, P.H., Katsounaros, I., and Koper, M.T.M. (2021). Electrocatalytic Nitrate Reduction for Sustainable Ammonia Production. Joule *5*, 290-294. https://doi.org/10.1016/j.joule.2020.12.025.

23. Wu, T., Sun, S., Song, J., Xi, S., Du, Y., Chen, B., Sasangka, W.A., Liao, H., Gan, C.L., Scherer, G.G., et al. (2019). Iron-facilitated dynamic active-site generation on spinel $CoAl_2O_4$ with self-termination of surface reconstruction for water oxidation. Nat. Catal. *2*, 763-772. https://doi.org/10.1038/s41929-019-0325-4.

24. Tang, C., and Qiao, S.Z. (2019). True or False in Electrochemical Nitrogen Reduction. Joule *3*, 1573-1575. https://doi.org/10.1016/j.joule.2019.06.020.

25. Li, Z., Cao, A., Zheng, Q., Fu, Y., Wang, T., Arul, K.T., Chen, J.L., Yang, B., Adli, N.M., Lei, L., et al. (2021). Elucidation of the Synergistic Effect of Dopants and Vacancies on Promoted Selectivity for CO_2 Electroreduction to Formate. Adv. Mater. *33*, e2005113. https://doi.org/10.1002/adma.202005113.

26. Seh, Z.W., Kibsgaard, J., Dickens, C.F., Chorkendorff, I., Norskov, J.K., and Jaramillo, T.F. (2017). Combining theory and experiment in electrocatalysis: Insights into materials design. Science *355*. https://doi.org/10.1126/science.aad4998.

27. Huang, Y., Long, J., Wang, Y., Meng, N., Yu, Y., Lu, S., Xiao, J., and Zhang, B. (2021). Engineering Nitrogen Vacancy in Polymeric Carbon Nitride for Nitrate Electroreduction to Ammonia. ACS Appl. Mater. Interfaces *13*, 54967-54973. https://doi.org/10.1021/acsami.1c15206.

28. Ye, S., Chen, Z., Zhang, G., Chen, W., Peng, C., Yang, X., Zheng, L., Li, Y., Ren, X., Cao, H., et al. (2022). Elucidating the activity, mechanism and application of selective electrosynthesis of ammonia from nitrate on cobalt phosphide. Energy Environ. Sci. *15*, 760-770. https://doi.org/10.1039/d1ee03097c.

29. Wang, Y., Xu, A., Wang, Z., Huang, L., Li, J., Li, F., Wicks, J., Luo, M., Nam, D.H., Tan, C.S., et al. (2020). Enhanced Nitrate-to-Ammonia Activity on Copper-Nickel Alloys via Tuning of Intermediate Adsorption. J. Am. Chem. Soc. *142*, 5702-5708. https://doi.org/10.1021/jacs.9b13347.

30. Liu, H., Timoshenko, J., Bai, L., Li, Q., Rüscher, M., Sun, C., Roldan Cuenya, B., and Luo, J. (2023). Low-Coordination Rhodium Catalysts for an Efficient Electrochemical Nitrate Reduction to Ammonia. ACS Catal. *13*, 1513-1521. https://doi.org/10.1021/acscatal.2c03004.

31. Han, S., Li, H., Li, T., Chen, F., Yang, R., Yu, Y., and Zhang, B. (2022). Ultralow overpotential nitrate reduction to ammonia via a three step relay mechanism. Preprint at Research Square. https://doi.org/10.21203/rs.3.rs-1550500/v1.

32. Zheng, W., Zhu, L., Yan, Z., Lin, Z., Lei, Z., Zhang, Y., Xu, H., Dang, Z., Wei, C., and Feng, C. (2021). Self-Activated Ni Cathode for Electrocatalytic Nitrate Reduction to Ammonia: From Fundamentals to Scale-Up for Treatment of Industrial Wastewater. Environ. Sci. Technol. *55*, 13231-13243. https://doi.org/10.1021/acs.est.1c02278.

33. De Luna, P., Hahn, C., Higgins, D., Jaffer, S.A., Jaramillo, T.F., and Sargent, E.H. (2019). What would it take for renewably powered electrosynthesis to displace petrochemical processes? Science *364*. https://doi.org/10.1126/science.aav3506.

34. McEnaney, J.M., Blair, S.J., Nielander, A.C., Schwalbe, J.A., Koshy, D.M., Cargnello, M., and Jaramillo, T.F. (2020). Electrolyte Engineering for Efficient Electrochemical Nitrate Reduction to Ammonia on a Titanium Electrode. ACS Sustain. Chem. Eng. *8*, 2672-2681. https://doi.org/10.1021/acssuschemeng.9b05983.
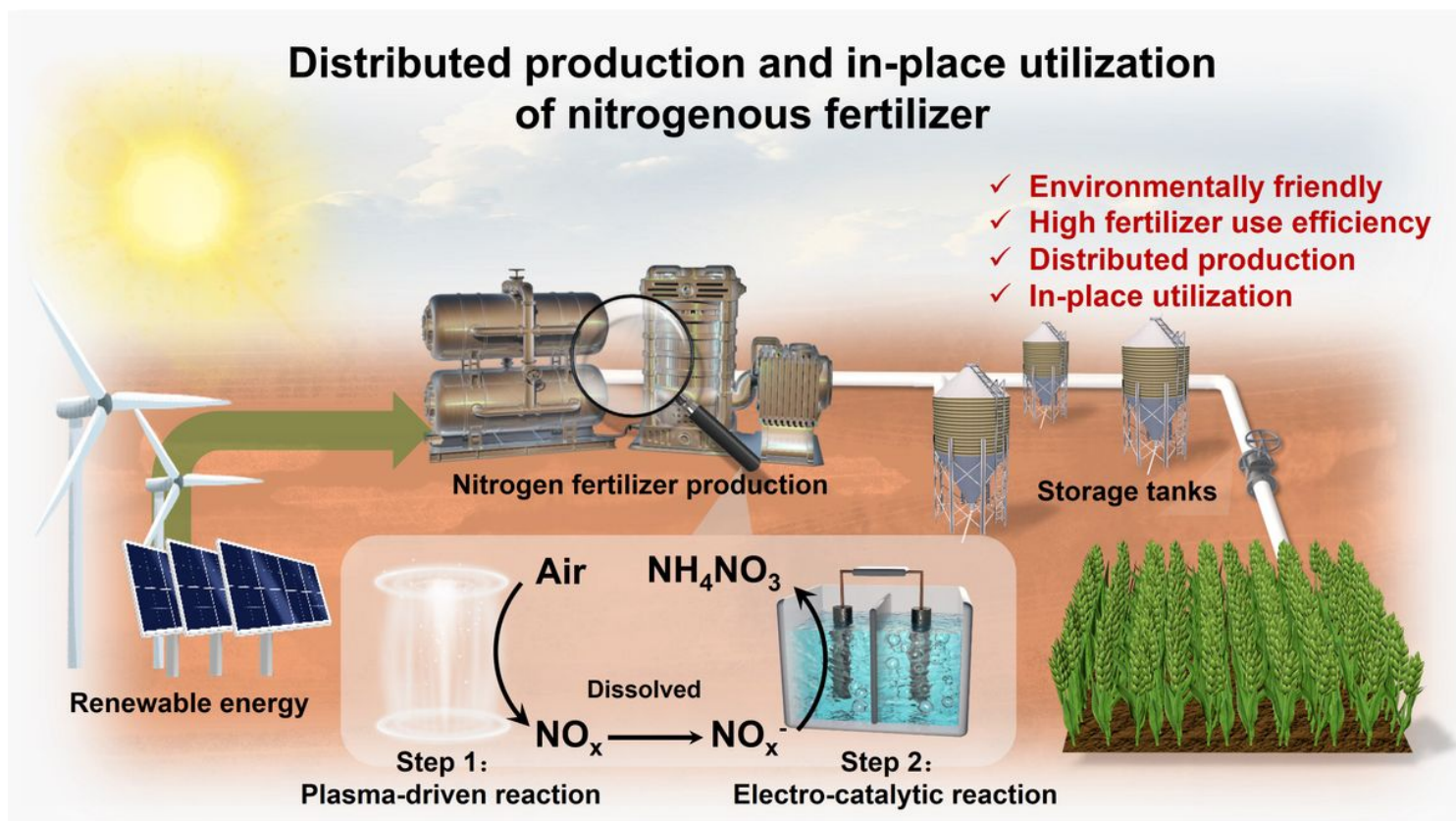
Figures

Figure 1

Schematic Illustration of the Two-Step Relay Strategy for Distributed Production and In-Place Utilization of a Liquid NH_4NO_3 Fertilizer

Figure 2

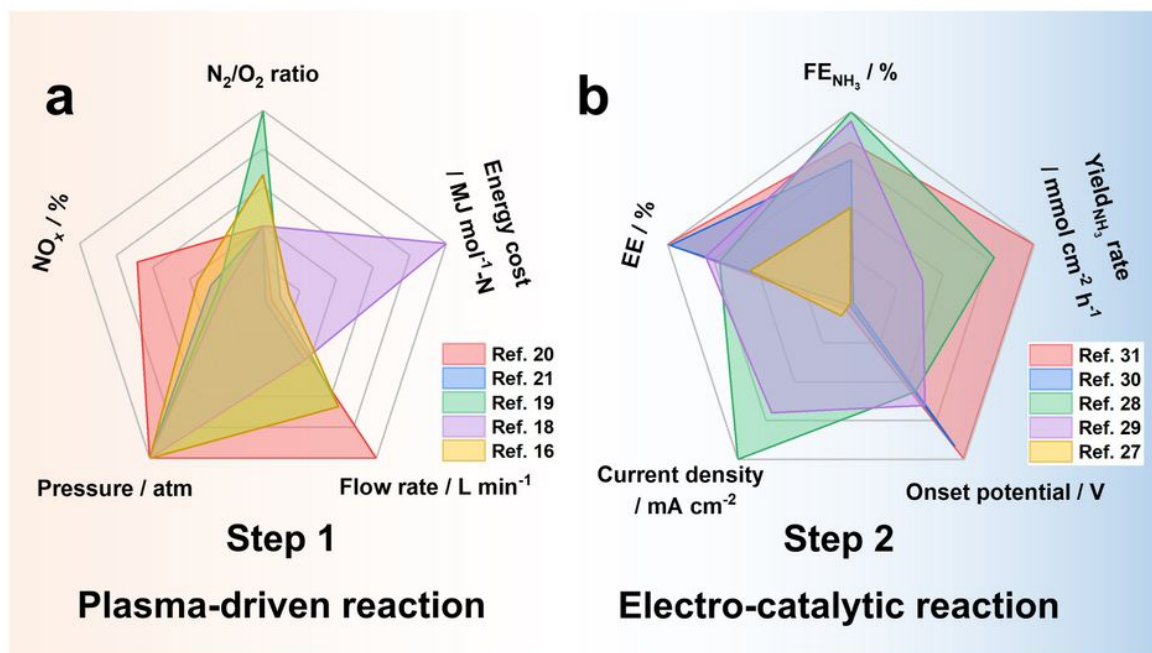Summary of Various Parameters for (a) Plasma-Driven NO_x Generation and (b) Electrocatalytic Nitrate Reduction to Ammonia
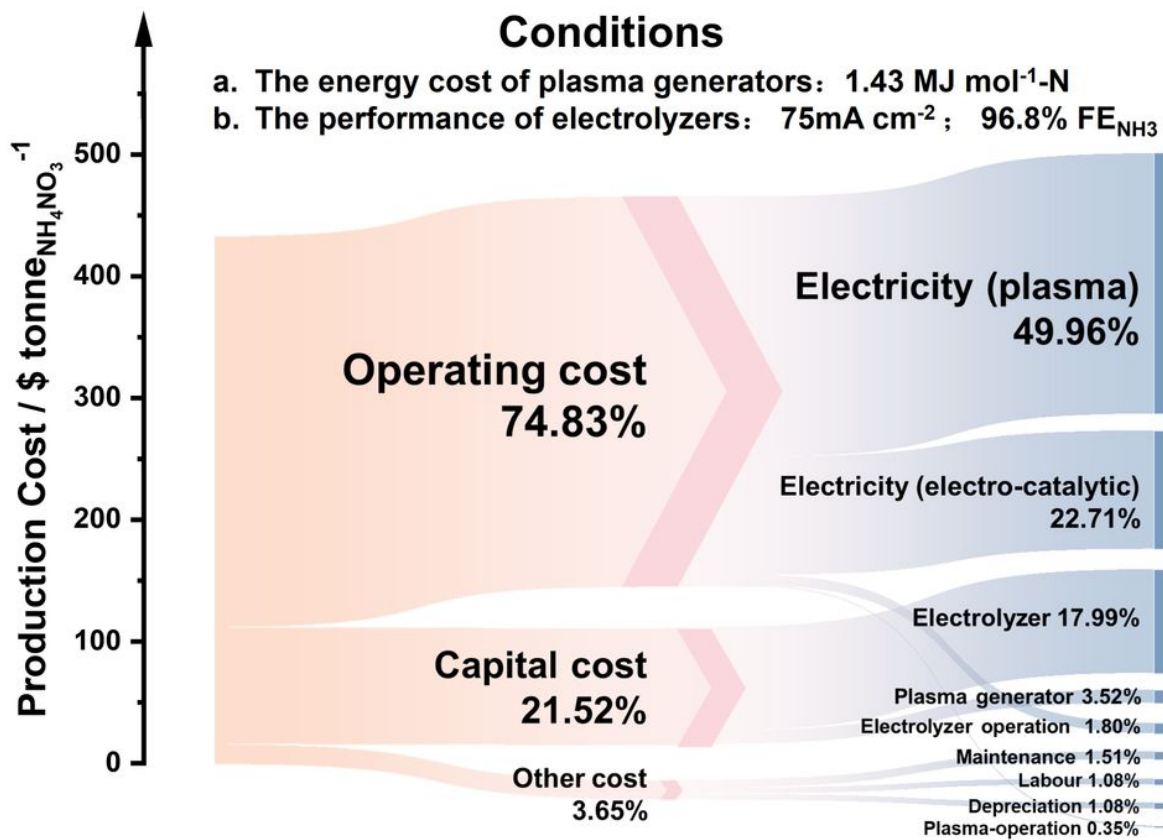
Conditions

a. The energy cost of plasma generators: 1.43 MJ mol^{-1}-N
b. The performance of electrolyzers: 75mA cm^{-2}; 96.8% FE$_{NH3}$

Production Cost / \$ tonne$_{NH_4NO_3}$$^{-1}$

Operating cost 74.83%

Capital cost 21.52%

Other cost 3.65%

Electricity (plasma) 49.96%

Electricity (electro-catalytic) 22.71%

Electrolyzer 17.99%

Plasma generator 3.52%
Electrolyzer operation 1.80%
Maintenance 1.51%
Labour 1.08%
Depreciation 1.08%
Plasma-operation 0.35%

Figure 3

The Subdivided Cost of the Entire Process for Liquid NH$_4$NO$_3$ Fertilizer Production at a Given Electricity Price of 2.21 cents kWh^{-1}